



**HAL**  
open science

# A passive thermal management system of Li-ion batteries using PCM composites: Experimental and numerical investigations

Mohamed Moussa El Idi, Mustapha Karkri, Mahamadou Abdou Tankari

## ► To cite this version:

Mohamed Moussa El Idi, Mustapha Karkri, Mahamadou Abdou Tankari. A passive thermal management system of Li-ion batteries using PCM composites: Experimental and numerical investigations. *International Journal of Heat and Mass Transfer*, 2021, 169, pp.120894. 10.1016/j.ijheatmasstransfer.2020.120894 . hal-04316599

**HAL Id: hal-04316599**

**<https://hal.u-pec.fr/hal-04316599v1>**

Submitted on 22 Jul 2024

**HAL** is a multi-disciplinary open access archive for the deposit and dissemination of scientific research documents, whether they are published or not. The documents may come from teaching and research institutions in France or abroad, or from public or private research centers.

L'archive ouverte pluridisciplinaire **HAL**, est destinée au dépôt et à la diffusion de documents scientifiques de niveau recherche, publiés ou non, émanant des établissements d'enseignement et de recherche français ou étrangers, des laboratoires publics ou privés.



Distributed under a Creative Commons Attribution - NonCommercial 4.0 International License

# A passive thermal management system of Li-ion batteries using PCMs composites: Experimental and numerical investigations

Mohamed Moussa EL IDI\*, Mustapha KARKRI, Mahamadou ABDOU TANKARI

Université Paris- Est, CERTES, 61 Av. du Général de Gaulle, 94010 Créteil Cedex, France.

Corresponding author: moussa.elidi@gmail.com

**Abstract** - This paper is dedicated to the design of an optimal thermal management system using a PCM-Metal Foam composite at the scale of a Li-ion batteries cells. To study the ability of a PCM and a PCM- Metal foam composite to absorb the heat generated by a Li-ion cell, a mathematical and numerical model was developed. The modeling is based on the data collected from characterizing experiments conducted with a new experimental test bench developed in the CERTES lab. In order to characterize the thermal behavior of Li-ion cell, the developed two-dimensional numerical model integrates the Brinkmann-Forchheimer-extended Darcy equation, the enthalpy-porosity method and two-temperature energy equations. The numerical study was made by coupling Matlab and COMSOL Multiphysics. The results showed that the addition of an aluminum foam allows a more efficient thermal management of the cell. The optimization study showed that an underestimation of the thickness (mass of PCM required) leads to extreme temperatures. It was also found that the addition of an extra volume of PCM does not have a great influence on the cell surface temperature.

**Keywords:** Phase change material (PCM), Battery Thermal Management System (BTMS), Numerical simulation, Metal foam, Li-ion.

$C_p$	Specific heat capacity, ( $J.kg^{-1}.K^{-1}$ )	$C$	Inertial coefficient, ( $W.m^{-2}.K^{-1}$ )
$\rho$	Density, ( $kg.m^{-3}$ )	$K$	Permeability, $m^2$
q	Heat flux	b	Liquid fraction
$L_f$	Latent heat of fusion ( $J.kg^{-1}$ )	subscripts	
$\mu$	Dynamic viscosity ( $Pa.s^{-1}$ )	s	Metal foam
t	Time, (s)	Li - ion	Li-ion cell
$\beta$	Thermal expansion of PCM, ( $K^{-1}$ )	f	fluid
T	Temperature, (K)	s	solid

$k$ 

Thermal conductivity, (W/m.K)

P

Phase change material

## 1. Introduction

To deal with the global warming and the increased energy demand caused by the rapid development as well as in industrial and developing countries, pure and hybrid electric vehicles (EVs/HEVs) with green power system sources, which are more environmentally friendly than conventional vehicles with combustion engines, are intensively designed and used. Li-ion batteries are the most commonly used in EVs/HEVs. They are selected because of their high specific energy density, good stability and low density. However, the battery lifespan, safe-use and performance are greatly impacted by the operating temperature. The maximum operating temperature of a Li-ion battery should not exceed 60 °C [1]. The performance of these batteries could be improved by thermal management to keep the temperature within a suitable operating range, between 15-35°C [2,3]. Therefore, a highly efficient Battery Thermal Management System (BTMS) is required to ensure that batteries operate under optimal conditions to improve performance and battery lifespan.

Several technologies are used to manage the thermal management of the batteries and avoid an excessive rise in temperature in the battery. There are two ways to decrease the battery temperature: internal modification at materials and chemistry of the battery to reduce the heat generation or external thermal management system to enhance the heat dissipation from the battery [4]. External management systems are air circuits, coolant circuit, heat pipes or the use of PCM and PCM composites [2,5]. Currently, external thermal management systems are the most widely used. The main problems with those systems are their cost, their complex implementation and their lack of reliability. Latent Heat Thermal Storage (LHTES), through the use of PCM, is an attractive way to achieve passive thermal management and ensure that the battery temperature remains within the desired range. PCMs have the ability to store and release a large amount of heat at the time of phase change in reduced volumes [6–8]. In fact, when the PCM is in the solid phase and the temperature rises to the melting temperature, it will become liquid and stores energy. Similarly, when it is in the liquid phase and the temperature drops below its melting point, it will become liquid again and releases the stored energy.

Li-ion batteries active thermal management systems can be classed into two main families: air circuits (natural or forced convection) and coolant circuits. Air circuits can be with or without heat exchanger. The forced convection circuits are the most widely used [2,5,9] for its high convective heat transfer coefficients. The advantages of these systems are direct access, low viscosity, light weight, simple configuration, low cost and easy maintenance. However, the specific heat capacity of the air is low. This limits its application for high flow rate operation and uniform air distribution, is difficult to achieve. Air cooling systems can be improved by the addition of fins. Coolant circuit for Li-ion battery thermal management are -generally- composed of a closed liquid circulation circuit, a pump to circulate the liquid and an exchanger to remove the amount of heat absorbed by the liquid [5]. The most commonly used liquids are water, glycols, oils and acetone [2,5,9]. Coolant circuit are more efficient than air cooling systems. Indeed, the liquids generally used have a higher specific heat capacity than air [2,10]. However, they are much more complex and expensive. They are also more expensive in terms of maintenance [2,11].

Li-ion battery passive thermal management systems can be classified into three groups: boiling liquid battery cooling [12–14], heat pipes [15] and PCM composites. In [16–19] the results show that heat pipes are capable of providing thermal management. However, this is not enough because the

temperature is still too high compared to the target of 25 °C as the maximum temperature the battery should reach.

The use of PCMs for thermal management of Li-ion batteries was first proposed in 2000 by Al-Hallaj and Selman [20]. They made a numerical study on the effect of the use of a PCM on the temperature field of a Li-ion battery. Their battery was composed of 8 cylindrical cells of 100 Ah. The authors compared the efficiency of used air circuit and passive management using PCM. The PCM used is paraffin RT55 with a melting temperature of about 56°C. The results for a 1C discharge at different discharge depths (DOD=0.25, 0.50, 0.75 and 1.0) showed that the use of PCM allows a more uniform temperature field compared to active air management by forced convection. In 2004, Khateeb et al [21] conducted a study on the thermal management of a Li-ion battery of an electric scooter by a PCM. Their battery pack composed of two modules of 18 cells of 12 Ah each. They studied charge-discharge cycles of 2.4C at different ambient temperatures (0°C, 30°C and 40°C). Three configurations have been studied: pure PCM, PCM-Metal Foam composite and the third one is a PCM-Metal Foam Composite with aluminum fins. The results of the numerical simulation showed that the addition of the metal foam and the aluminum fins is necessary to keep the battery temperature within the desired range of temperature for three consecutive cycles. The results also highlighted the importance of the melting temperature. These results are in agreement with other results in the literature [21]. In 2005, the Al-Hallaj team published several studies on the use of PCMs for thermal management of Li-ion batteries [22,23]. In 2008, Sabbah et al [24] conducted an experimental and numerical study which aimed to compare an active management system with a passive management system. It was a system of a forced convection and a passive management system by a PCM of melting temperature between 52-55°C. Their test device was composed of 68 modules of 20 cells (3.7 and 1.5Ah) of batteries. The study was carried out under two ambient temperatures, 25°C and 45°C. In the case of cooling by an air circuit, several speeds were studied. Experimental results showed that in the extreme conditions, Fast charging with high ambient temperature, the thermal management by the PCM is more efficient than the forced air circuit. In 2010, Duan et al [25] published an experimental study on the use of a PCM for the thermal management of a Li-ion battery. They replaced electric batteries by heated cylindrical casings. The PCM has a melting temperature of 50°C. Three experiments were conducted. Several experiments were performed by the authors. The results showed that the use of PCM allows to reduce the temperature peak and to have a more uniform temperature distribution in the battery. These results are in good agreement with other studies in the literature [2,5,26].

All these studies confirm that PCMs allow to decrease the temperature of Li-ion batteries and to have an uniform temperature field in the battery or pack of batteries. BTMS using PCM is hampered by two main problems: the first is their low thermal conductivity and the second is the regeneration (evacuation of the stored heat). The thermal conductivity of PCMs can be improved by adding expanded graphite or by incorporation into metal foam. In particular, metal foams have specific characteristics such as high porosity (porosity between 0.8 and 0.98), high thermal conductivity and a large contact area. This qualifies them to be a good solution to improve the heat exchanges of MCP-metal foam composites [27].

From 2014, several researchers have studied numerically and experimentally, the use of PCM-Metal Foam [28] and Expanded Graphite (EG)-PCM composites in order to solve the problems of passive thermal management by a pure PCM mentioned before. In [29], the authors conducted an experimental study of the efficiency of Li-ion batteries thermal management by comparing a pure PCM and a PCM-Metal foam composite. The PCM used is paraffin RT 44HC with melting temperatures of 42°C and 49°C. The foam used is a copper foam. The cells (battery) have a capacity of 10 Ah. The thermal behavior of the battery was followed for discharge cycles of 0.5C, 1C and 3C at an ambient temperature of 25°C. The results showed that the addition of copper foam allows lower

temperatures with a more uniform temperature field. In [30] an experimental and numerical study on the thermal management of a Li-ion battery by an expanded paraffin-graphite composite was conducted. Different types of paraffin with different melting temperatures 36°C, 44°C and 52°C were tested. The authors replaced the cells by heating elements that reproduce the same thermal behavior of the cells. The objective was to keep the cell temperature below 50°C. The ambient temperature is 27°C. The results showed that the PCM composite with a high or low phase-change temperature are not suitable for battery thermal management system. Several works on BTMS using PCM composite were published after [31]. More recently Xiao et al [32] in order to resolve thermal stability problem of PCM for BTMS designed a new PCM (polymer PCM) with ultra-high thermal stability incorporated with EG. The results showed an excellent stable heat dissipation performance.

Recently, some efforts have been focused on the study of hybrid systems for the Li-ion batteries thermal management by adding an active system designed at a minimum power in order to solve the problems of passive thermal management by a pure PCM composite [33–39]. Mashayekhi et al [38] proposed hybrid system using PCM and nanofluid in minichannels. A paraffin with melting temperature between 42°C- 44°C incorporated in copper foam was used as passive system. Aluminum minichannel containing coolant (Al<sub>2</sub>O<sub>3</sub> nanofluid) flow was considered as the active part of BTMS. The thermal response of Li-ion batteries in high discharge rates was investigated by the authors. They concluded that passive system was inefficient to keep the battery temperature below the safety limit (60 °C) in high discharge rates. The results showed –also- that the use of nanofluid can reduce the maximum temperature reached by batteries by 15.5% in active system case and 8.5% in hybrid system case. In [35] Mehrabi-Kermani et al conducted an experimental study on the use of a novel hybrid system for Li-ion batteries thermal management. Paraffin/ Copper foam composite integrated with a heat-sink air cooling was used. The results showed that the active and passive systems were ineffective in hot climate (40 °C). This is because the melting of the used paraffin starts at 37.8 (below 40°C). Bamdezh and Molaieimanesh [34] conducted a numerical study on the thermal performance of hybrid system for Li-ion batteries thermal management. An air cooling system was used as an activate TMS and an embedded PCM as a passive TMS. The results showed that the maximum temperature difference of the studied battery does not exceed 1.5°C. Lv et al [39] inspired by Tesla cooling system, proposed a novel BTMS using serpentine PCM coupled with forced air convection. They found that the proposed system can reduce the used PCM composite weight by ~70% and increasing the energy density of the battery module from 107.8 to 121.6 Wh kg<sup>-1</sup>.

**Table 1** summarizes the advantages and drawbacks of different Li-ion batteries thermal management systems.

	Advantages	Drawbacks
Natural convection	<ul style="list-style-type: none"> <li>• No energy consumption</li> <li>• Simplicity</li> <li>• No operational costs</li> <li>• Low initial cost</li> <li>• Passive cooling</li> </ul>	<ul style="list-style-type: none"> <li>• Low heat transfer coefficient</li> <li>• High impact of ambient air temperature</li> <li>• Limited temperature reduction</li> <li>• Uneven temperature distribution</li> <li>• Insufficient for high discharge rates</li> </ul>
Forced Convection	<ul style="list-style-type: none"> <li>• Simplicity</li> <li>• Low initial cost/ Low maintenance</li> </ul>	<ul style="list-style-type: none"> <li>• Low heat transfer coefficient</li> <li>• High impact of ambient air temperature</li> <li>• Energy consumption (fans)</li> <li>• Uneven temperature distribution</li> <li>• Low efficiency</li> <li>• Insufficient for extreme conditions</li> </ul>
	<ul style="list-style-type: none"> <li>• More intensive heat transfer</li> </ul>	<ul style="list-style-type: none"> <li>• Complexity</li> </ul>

Coolant circuit	<ul style="list-style-type: none"> <li>• More uniform temperature distribution</li> <li>• Increased efficiency</li> </ul>	<ul style="list-style-type: none"> <li>• Energy consumption (pumps)</li> <li>• High initial cost/ High operational cost</li> <li>• Leakage risks</li> <li>• Short lifespan</li> <li>• Insufficient for extreme conditions</li> </ul>
Heat pipe	<ul style="list-style-type: none"> <li>• Improvement of thermal conductivity</li> <li>• Improved heat transfer</li> <li>• Increased efficiency</li> </ul>	<ul style="list-style-type: none"> <li>• Complexity</li> <li>• Highest initial cost/ High operational cost</li> <li>• Leakage risks</li> <li>• Energy consumption</li> </ul>
PCM	<ul style="list-style-type: none"> <li>• Passive cooling</li> <li>• Low cost/ Low maintenance</li> <li>• Increased efficiency</li> <li>• More uniform temperature distribution</li> <li>• Playing in extreme conditions</li> </ul>	<ul style="list-style-type: none"> <li>• Low thermal conductivity</li> <li>• Regeneration of the PCM</li> <li>• Overcooling</li> <li>• Volume expansion/ risks of Leakage</li> </ul>
PCM- Metal foam & PCM- EG composites	<ul style="list-style-type: none"> <li>• High thermal conductivity</li> <li>• Passive cooling</li> <li>• Increased efficiency</li> <li>• Low cost/ Low maintenance</li> <li>• More uniform temperature distribution</li> <li>• Playing in extreme conditions</li> </ul>	<ul style="list-style-type: none"> <li>• Regeneration of the PCM</li> <li>• Overcooling</li> <li>• Volume expansion/ Leakage risks</li> </ul>
Hybrid system	<ul style="list-style-type: none"> <li>• High efficiency</li> <li>• More uniform temperature distribution</li> <li>• Playing in extreme conditions</li> <li>• Increased heat transfer</li> </ul>	<ul style="list-style-type: none"> <li>• Initial cost</li> <li>• Complexity</li> <li>• Volume expansion (PCM)/ Risk of leakage</li> <li>• Energy consumption</li> </ul>

**Table 1:** *Advantages and Drawbacks of different Li-ion batteries thermal management systems*

The majority of studies carried out focus on maintaining the temperature of the batteries in a temperature range between 40°C and 60°C. However, the optimal temperature range is between 15°C and 35°C [3,40], depending on the manufacturer [2] (Figure 1). Few studies in the literature have studied the sizing and optimization of the amount of PCM used to manage the temperature of a Li-Ion cell [41]. In this paper we are interested in the study of Li-ion cell thermal behavior and in the designing and optimization of a passive management system by a PCM-metal foam composite. The goal is to keep the cell at a temperature above 27°C under a 1C charge/ discharge rate. A new platform will be presented and described. The first part will be devoted to the presentation of the platform and to the study the battery thermal behavior. It allows to study the temperature evolution of a Li-ion cell and its heat flux released during a charge/ discharge cycle. The actual heat dissipated by the cell has been calculated from the experimental results and by used the trapezoidal rule. A MATLAB code was used to compute the heat dissipated by the cell. The numerical simulation of the thermal behavior of the PCM and the PCM-metal foam composite is done under COMSOL Multiphysics and Matlab. The results will be presented and discussed.

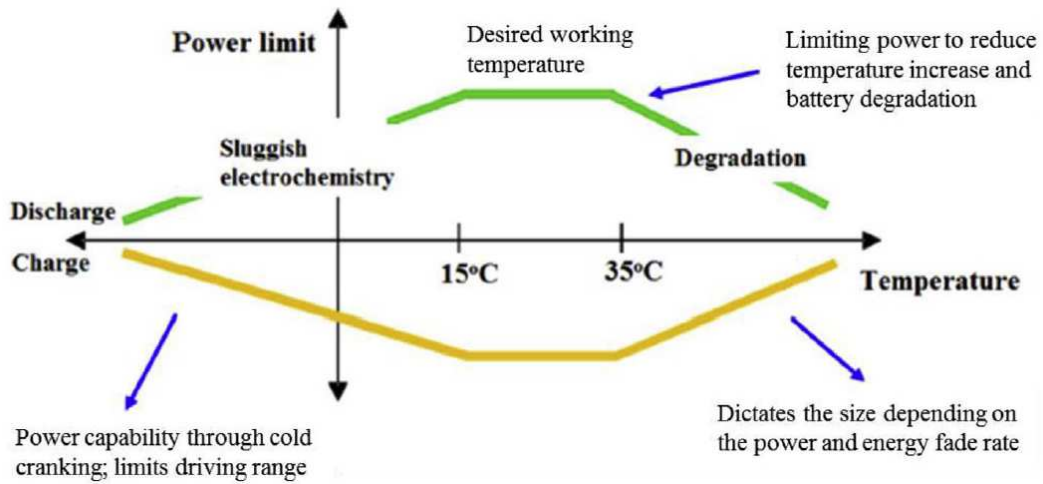


Figure 1: Battery power curves (charge/ discharge) depending on the temperature [3]

## 2. Experimental device

The experimental test bench developed in this paper used to charge and discharge the 18650 cell with a capacity of 2500 mAh is shown in *Figure 1*. The cell is connected to a DC power supply which ensures the battery charge and to an active charge which ensures the discharge. The electrical and geometrical characteristics of the cell provided by the manufacturer. The used Li-ion cells, supplied by the company VARTA, are cylindrical with dimensions:  $r=9.255\text{mm}$ ;  $H=70\text{mm}$ . *Figure 2 (a)* shows a picture of the cell used in the present study. Electromechanical relays are inserted to open and close the electrical circuit. In order to follow the temperature evolution of the cell, two T-type thermocouples are placed at different locations on the surface of the cell. *Figure 2 (c)* shows the positioning of the thermocouples. A cylindrical sensor encapsulates the cell to measure the heat flow dissipated by the cell. A LabVIEW program is developed for battery charge/discharge cycles. It is used to control the relays, power supply and active load as well as the acquisition of the measured data. The instrumented cell is placed in a climate chamber to control the ambient temperature and humidity. The studied cell is suspended by its power cables in order to avoid thermal exchanges by conduction between the battery surface and the external environment, *Figure 3*.

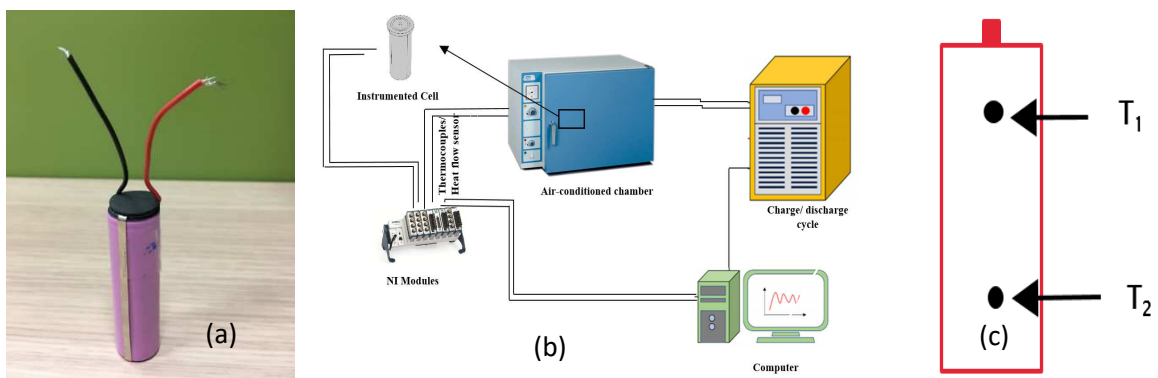


Figure 2: Experimental testbed

- a) Sample of battery cell ; b) synoptic of the testbed; c) locations of thermocouples.

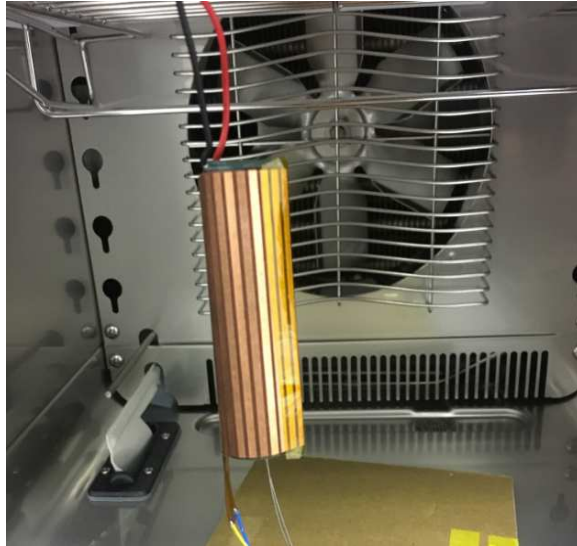


Figure 3: Instrumented cell in climatic chamber

### 3. Experimental study

#### 3.1. Test procedures

The tests were carried out for different currents and for a maximum voltage of 4V and without pause between two consecutive cycles. A cycle corresponds to a charge followed by a discharge. Figure 4, shows the voltage and current profiles for a 1C-test (2.5 A). This means that if the battery, fully charged, is discharged by a current rate of 2.5 A, it will reach its stop voltage after one hour of discharge. The tests are stopped once the steady state is reached as shown in Figure 5. Indeed, the temperature rises at the beginning and tends towards a constant value that characterizes the steady state.

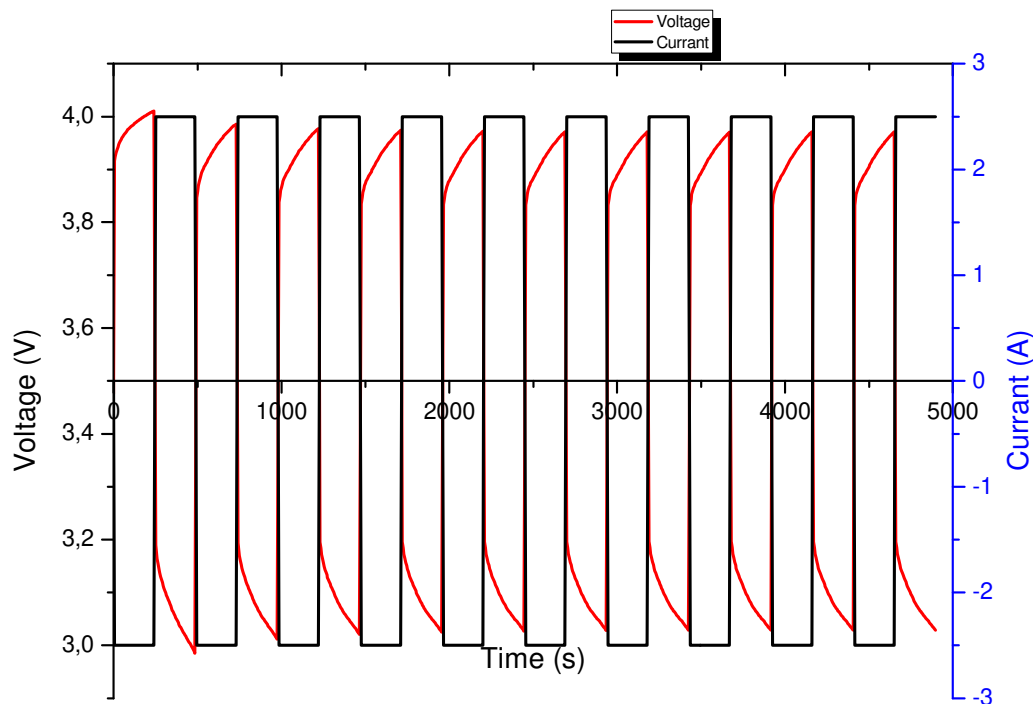


Figure 4: Charge/discharge profile

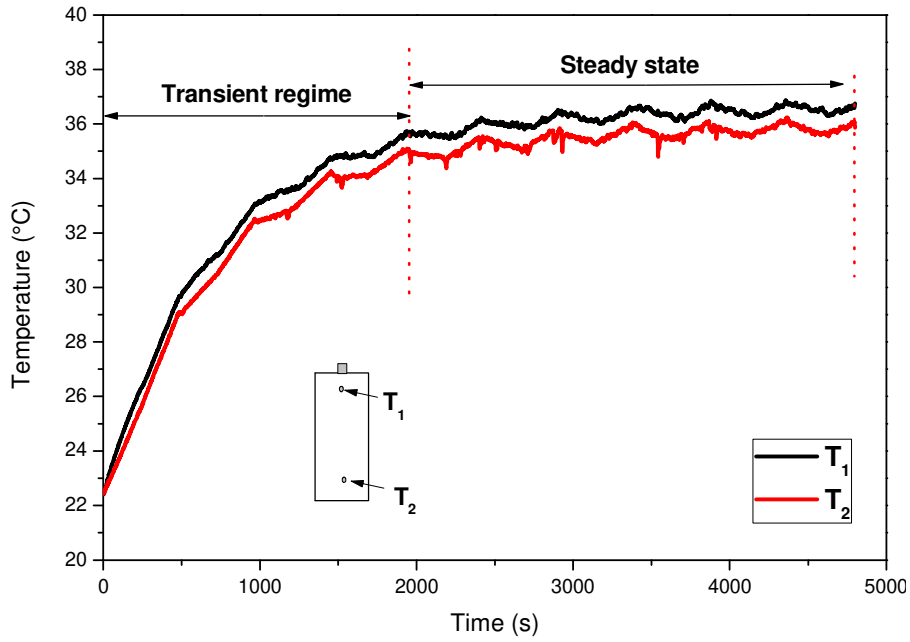


Figure 5: Temperature evolution on the cell surface

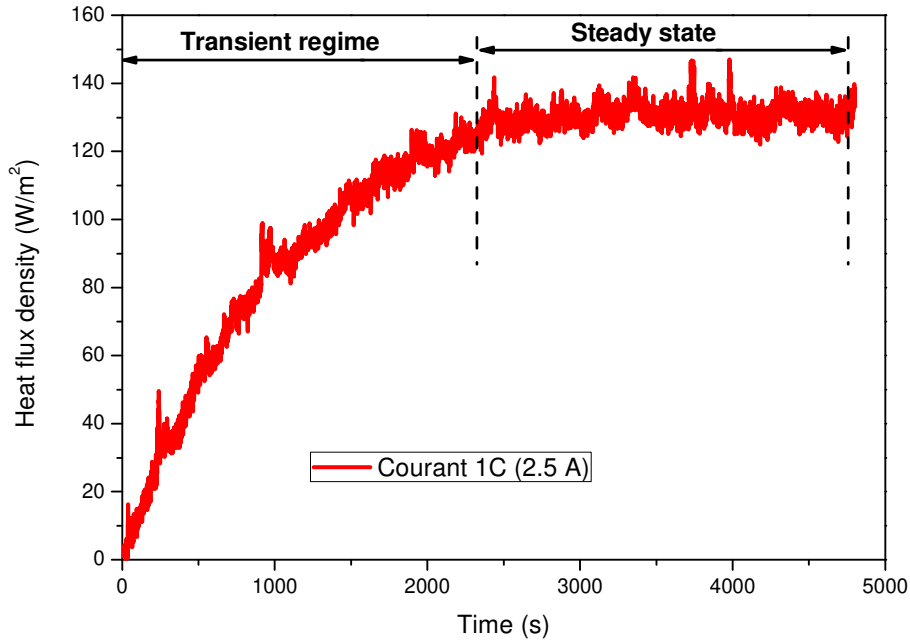


Figure 6: Evolution of the heat flux density on the lateral reell surface

### 3.2. Evolution of the temperature and heat flux density of the cell

The cell surface temperature and heat flux are essential to estimate the performance, size and PCM mass of the cooling system. *Figure 5* shows the evolution of the cell surface temperature for a charge/discharge cycle at 1C (2.5A). Two sources are involved in the generation of heat in a battery. The first is generated by the Joule effect, considered as an irreversible source, and the second source is a reversible, which corresponds to the heat produced at the interface between the electrolyte and the electrodes, is of thermodynamic origin [15,26,42,43]. Overall we observe in this figure a slight decrease

in temperature during charging and also an increase during discharge. It can be seen that at the end of the cycle, the heat absorbed by the reaction during charging is fully restored during discharge. This reversible phenomenon is due to the variation in entropy caused by the insertion/disinsertion of Li<sup>+</sup> ions in the crystal structure of the active material of the negative electrode. **Figure 5** show a temperature difference of 0.4°C between temperatures T<sub>1</sub> and T<sub>2</sub> measured by thermocouple 1 and 2. This means that the cell surface temperature is not homogenous. **Figure 6** shows the evolution of the surface heat flux density of the cell. We notice that the profile obtained at the same rate as the temperature. One clearly distinguishes the transition zone and the permanent zone.

### 3.3. Study of the influence of charge/discharge current on cell temperature

In order to investigate the impact of current rates on the cell surface temperature, three current rates were investigated, 1C, 2/5C and 4/5C. **Figure 7** shows the temporal cell surface temperature evolution measured by thermocouple T<sub>1</sub> as a function of the current rates. The temperature inside the air-conditioned chamber is fixed at 22.5°C. It can be observed that the cell surface temperature increases with the current rates. The maximum temperature reached for the three current rates investigated in the present study is 36°C, 33°C and 26°C for respectively 1C, 2/5C and 4/5C. The cell surface temperature difference between current rate of 4/5C and 1C can reach 10°C. Indeed, both reversible and irreversible heat sources are dependent on the solicitation current. The results found in this study for cell 18650 are in agreement with the results found by R. Rizk et al [43]. In [43] the authors studied the thermal behavior of a high capacity prismatic Li-ion battery.

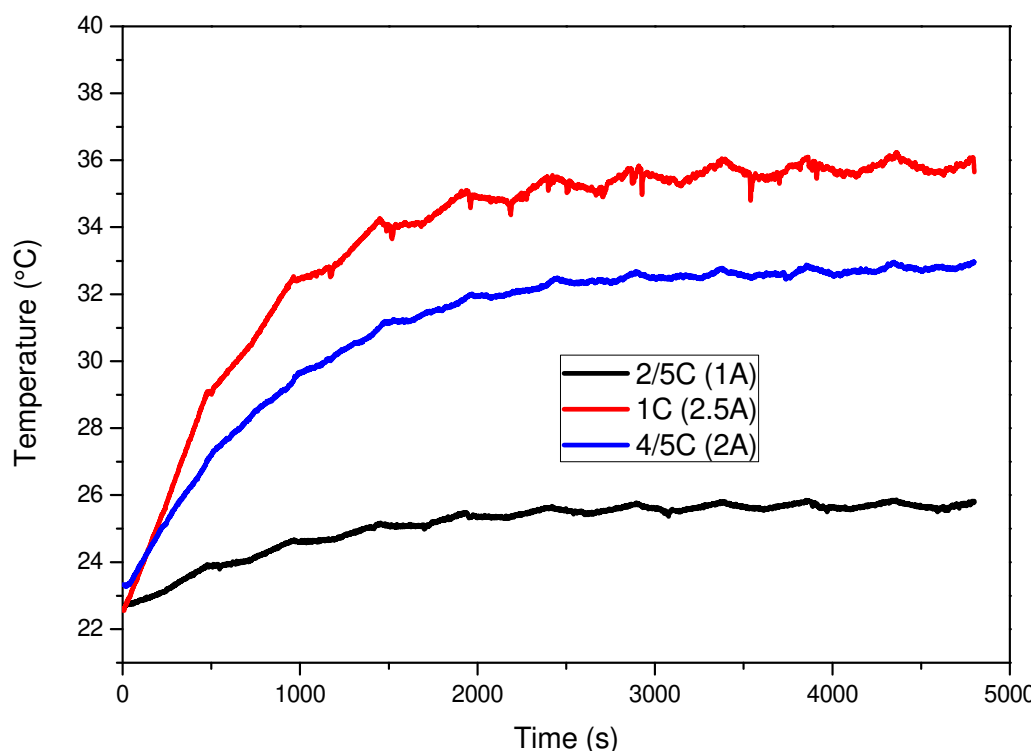


**Figure 7:** Influence of the current rates on the cell surface temperature evolution

### 3.4. Study of the impact of charge/ discharge cycle time on the steady state temperature

In this section we study the influence of charge/ discharge cycle time on the temperature in steady state. All the tests are done in 4/5C regime, i.e. with a current of 2A. It is clear that the charge/ discharge cycle time has a great impact on the temperature peak. Indeed, a longer load time leads to higher entropy and subsequently to higher temperatures. Our choice is made to study with a the charge/ discharge cycle time of 8 minutes.

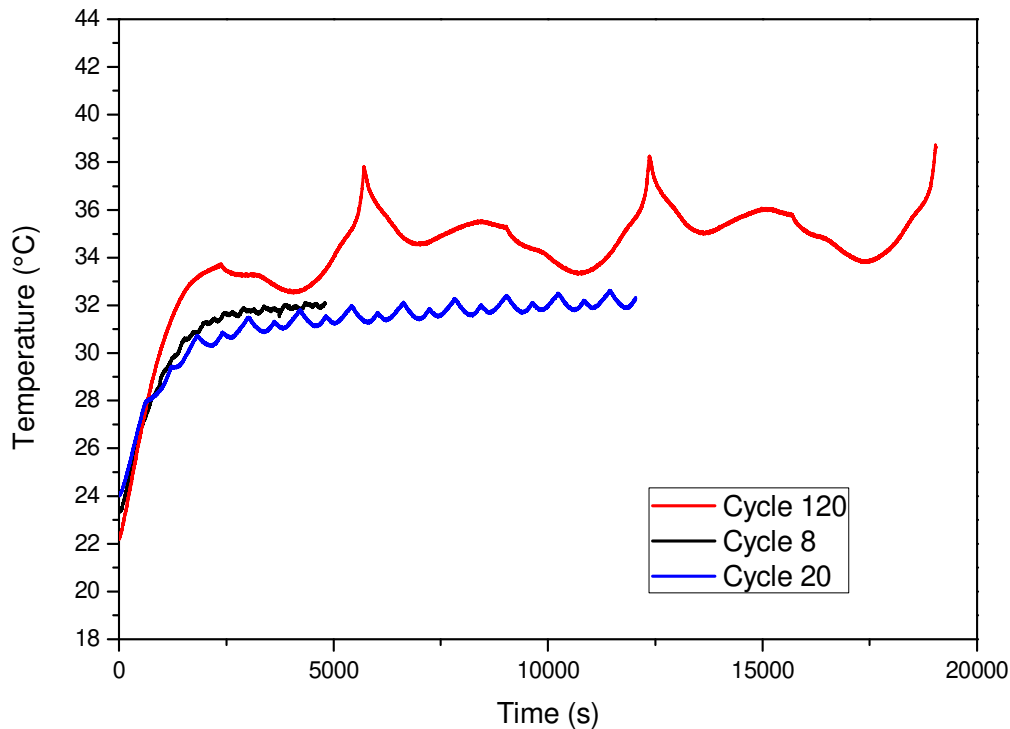
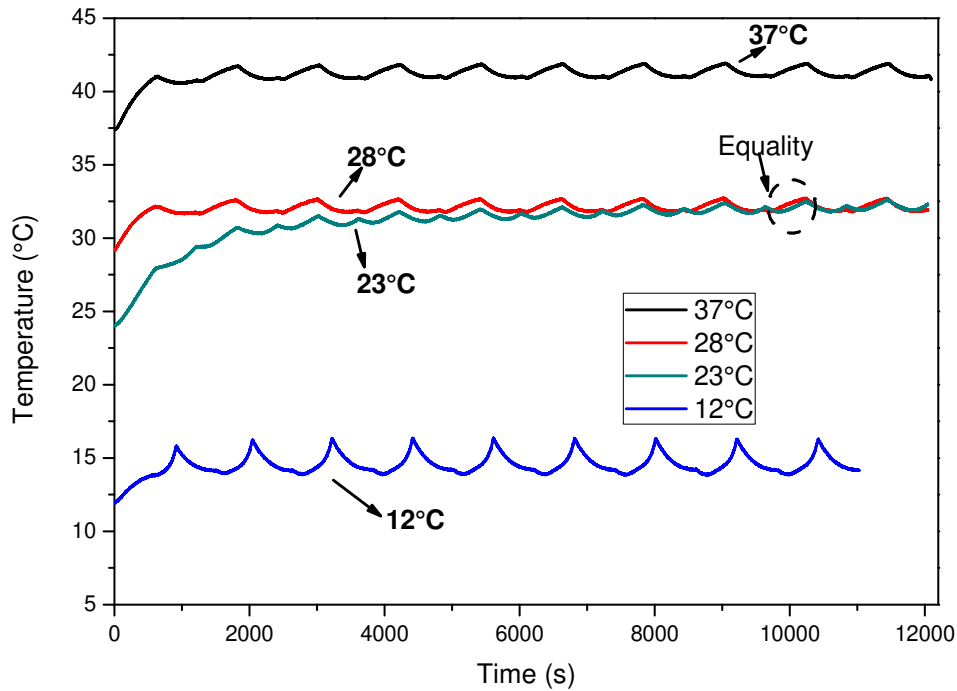


Figure 8: Influence of the charge/ discharge cycle time on the cell temperature

### 3.5. Study of the influence of the ambient temperature on the cell surface temperature

In order to study the impact of the ambient temperature on the temporal evolution of the cell temperature. The air-conditioned enclosure allows us to impose a constant temperature within the air-conditioned enclosure. Four temperatures were studied: 12°C, 23°C, 28°C and 37°C. All the tests were made in 4/5C regime (2A). The results show that in the case of ambient temperatures of 23°C and 28°C, the temperature of the cell converges to the same temperature. This demonstrates that a difference in ambient temperature 5°C between 23°C- 28°C does not have a great impact on the cell temperature without BTMS. On the other hand, in the case of a BTMS with a PCM, such a difference can have a big impact if the melting temperature is in this temperature interval. For example a BTMS with paraffin RT27.



*Figure 9:* Influence of the ambient temperature

The study of the Li-ion cell thermal behavior showed that it is affected by several parameters: Current rate, Charge/ discharge cycle type and ambient temperature. A general thermal management system cannot be designed. For this reason, we have chosen to focused on the designed and conception for a thermal management system with the follow conditions: current rate (1C), frequently of cycle 20 minutes and ambient temperature 22°C. The goal is to keep the temperature of the cell lower than 27°C.

## 4. Thermal management using PCM-Metal Foam Composite

In this section we are interested in the designing and optimization of a passive management system using a PCM-metallic foam composite. The goal is to keep the cell at a temperature above 27°C under a 1C current rate. The actual heat dissipated by the cell has been calculated from the experimental results presented earlier in this manuscript and thanks to a calculation code developed under Matlab. COMSOL Multiphysics and Matlab are used to simulate the thermal behavior of the PCM and the PCM-metal foam composite used to absorb the heat released by the cell.

### 4.1. Modeling method

#### 4.1.1. Physical model

To simplify numerical simulations, the problem is considered in bidimensionnel (2D). The physical model is shown in **Figure 10**. **Figure 11** present a simplified physical model with boundary conditions. It is a Li-ion cell surrounded either by a pure PCM or by a PCM-metal foam composite. It is an aluminum foam with a porosity of 0.93 and a pore density of 40PPI. The choice of this foam with these characteristics is based on our work in [44] where we studied the impact of the thermal characteristics and the morphology of the foam on the solid-liquid phase change kinetics of a PCM incorporated in a high porosity metal foam. The external walls are considered adiabatic. Our choice for the PCM is the

RT27 paraffin. The choice of the RT27 paraffin is justified by its melting temperature around 27°C. The proprieties of paraffin RT27 and the aluminum foam used for the present study are given in **Table 2**.

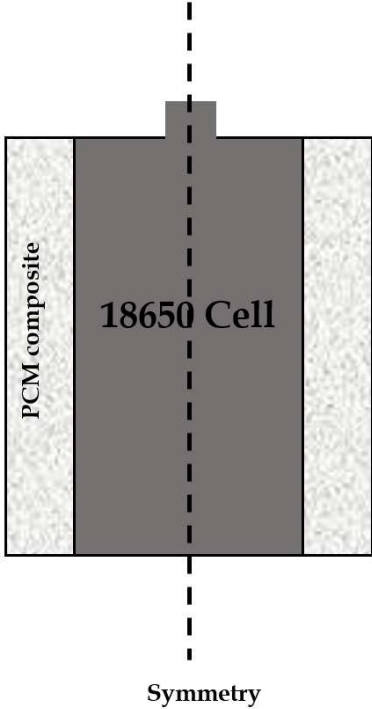


Figure 10: Physical model

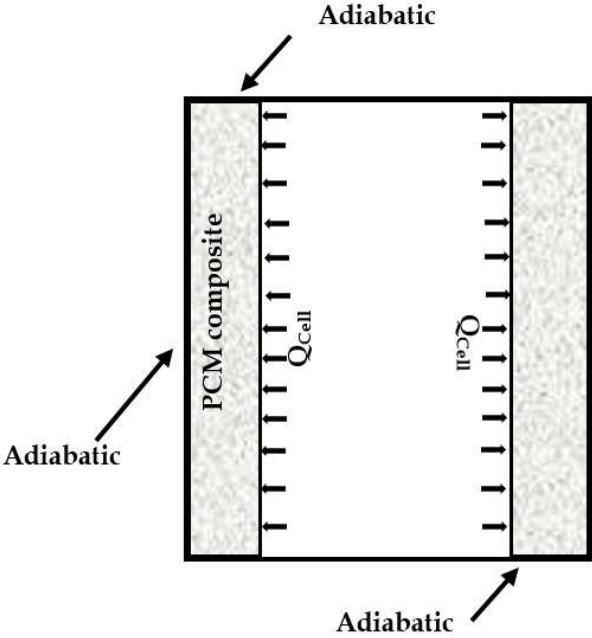


Figure 11: Simplified physical model with boundary conditions

properties	Paraffin RT27	Aluminu m	Paraffin RT58
Density ( $kg.m^{-3}$ )	870	2800	850
Heat capacity-solid ( $J.K^{-1}.kg^{-1}$ )	2400	910	2100
Latent heat ( $KJ.kg^{-1}$ )	179		181

Melting temperature (K)	300.15	331.15
Dynamic viscosity ( $Kg.m^{-1}.s^{-1}$ )	$3.42 \times 10^{-3}$	0.0269
Thermal conductivity -solid ( $W.K^{-1}.m^{-1}$ )	0.24	237
1)		
Density - liquid ( $kg.m^{-3}$ )	760	775
Heat capacity -liquid ( $J.K^{-1}.kg^{-1}$ )	1800	2100
Thermal conductivity - liquid ( $W.K^{-1}.m^{-1}$ )	0.15	0.2
1.m <sup>-1</sup> )		
$\beta$ ( $K^{-1}$ )	$0.5 \times 10^{-3}$	$1.1 \times 10^{-4}$

**Table 2:** Thermophysical properties of paraffin RT27, RT58 and aluminum foam.

#### 4.1.2. Assumptions

- The liquid is considered as incompressible and the flow is laminar.
- The natural convection caused by buoyancy is subject to the Boussinesq approximation.
- The thermal radiation is neglected in the metal foam during melting and solidification.
- The metal foam is considered as isotopic and homogeneous.
- The volume expansion is neglected.

#### 4.1.3. Thermophysical and structural proprieties of metal foam

Thermophysical proprieties of aluminum foam used in this study are presented in **Table 2**. Many researches have been carried out to develop an analytical model for predicting permeability and the inertial coefficient of metal foam [27-33]. In this work, we use the model of Calmidi [28] to calculate permeability and the inertial coefficient.

Permeability:

$$K = 0.00073d_p^2(1-\varepsilon)^{-0.224} \left( \frac{d_f}{d_p} \right)^{-1.11} \quad (1)$$

Inertial coefficient:

$$C = 0.00212d_p^2(1-\varepsilon)^{-0.132} \left( \frac{d_f}{d_p} \right)^{-1.63} \quad (2)$$

Where  $d_f$  denotes the equivalent diameter of metal foam fibers and  $d_p$  pores diameter [28]:

$$\frac{d_f}{d_p} = 1.18 \sqrt{\frac{1-\varepsilon}{\pi}} \left( \frac{1}{1-e^{-(1-\varepsilon)/0.04}} \right) \quad (3)$$

$d_p$  can be calculate from pore density:

$$d_p = \frac{0.0254}{PPI} \quad (4)$$

The specific area  $a_{PS}$  can be calculated by the following formula [29].

$$a_{PS} = \frac{3\pi d_f (1-e^{-(1-\varepsilon)/0.04})}{(0.59d_p)^2} \quad (5)$$

#### 4.1.4. Mathematical model

Continuity equation:

$$\frac{\partial u}{\partial x} + \frac{\partial v}{\partial y} = 0 \quad (6)$$

Momentum equations:

$$\frac{\rho_p}{\varepsilon} \frac{\partial u}{\partial t} + \frac{\rho_p}{\varepsilon^2} (\vec{V} \vec{\nabla}) \cdot u = -\frac{\partial p}{\partial x} + \frac{\mu}{\varepsilon} \nabla^2 u - \left( \frac{\mu}{K} + \frac{\rho_p C}{\sqrt{k}} |u| \right) u + S_u \quad (7)$$

$$\frac{\rho_p}{\varepsilon} \frac{\partial v}{\partial t} + \frac{\rho_p}{\varepsilon^2} (\vec{V} \vec{\nabla}) \cdot v = -\frac{\partial p}{\partial y} + \frac{\mu}{\varepsilon} \nabla^2 v - \left( \frac{\mu}{K} + \frac{\rho_p C}{\sqrt{k}} |v| \right) v + S_v + \rho_p g \beta (T - T_{ref}) \quad (8)$$

Where  $S_u = A \frac{(1-b)^2}{B^3 + b} u$ , and  $S_v = A \frac{(1-b)^2}{B^3 + b} v$  denoted the source term to damping the velocity in solidified phase ( $A$  and  $B$  are two constants). They are deduced from Carmen-Kozney relation [45]. In this study we take  $A=10^5$  and  $B=10^{-3}$ . For the solidified phase,  $b = 0$  leads the item to be infinity to damp the velocity in the momentum equation. For fluid phase,  $b = 1$  leads the item to be zero.

$b(T)$  can be defined as:

$$b(T) = \begin{cases} 0 & T < (T_m - \Delta T / 2) \\ \frac{T - T_m + \Delta T / 2}{\Delta T} & (T_m - \frac{\Delta T}{2}) \leq T < (T_m + \frac{\Delta T}{2}) \\ 1 & T > (T_m + \Delta T / 2) \end{cases} \quad (9)$$

The dynamic viscosity is modified by using  $S(T) = A \frac{(1-b)^2}{B^3 + b}$  to have an extremely high value when the PCM is at a temperature below its melting temperature.

$$\mu_p(T) = \rho_{pl} (1 + S(T)) \quad (10)$$

For non-equilibrium thermal condition, two energy equations are used for PCM and aluminum foam as following:

Energy equation for PCM:

$$\varepsilon \rho_p C_p \frac{\partial T_f}{\partial \tau} + \rho_p C_p (u \frac{\partial T_p}{\partial x} + v \frac{\partial T_p}{\partial y}) = k_p \nabla^2 T_p + h_{ps} a_{ps} (T_s - T_p) \quad (11)$$

The density variation of PCM can be given by:

$$\rho_p(T) = \rho_{ps} + (\rho_{pl} - \rho_{ps}) b(T) \quad (12)$$

The phase change temperature interval is taken at 3°C [46]. The specific heat of PCM can be written as [47,48]

$$C_{pp} = C_{ps} + (C_{pl} - C_{ps}) b(T) + L_f D(T) \quad (13)$$

Where  $L_f$  is the latent heat of fusion:

$$D(T) = e^{\left( \frac{-(T-T_m)^2}{\left( \frac{\Delta T}{4} \right)^2} \right)} \sqrt{\pi \left( \frac{\Delta T}{4} \right)^2} \quad (14)$$

$D$  is a smoothed Delta Dirac function which is zero everywhere except in the interval. Its integral is equal to 1. The use of this function ensures that the latent heat is conserved during the melting process. The thermal conductivity of PCM can be given as:

$$k_p(T) = k_{p_s} + (k_{p_l} - k_{p_s}).b(T) \quad (15)$$

Energy equation for metal foam:

$$(1 - \varepsilon)\rho_s c_{p_s} \frac{\partial T_s}{\partial \tau} = k_s \nabla^2 T_s - h_{p_s} a_{p_s} (T_s - T_p) \quad (16)$$

Where  $k_{p_e}$ ,  $k_{s_e}$ ,  $h_{p_s}$  are the effective thermal conductivity of paraffin, effective thermal conductivity of metal foam and the interstitial heat transfer coefficient between the porous metallic surface and saturating PCM. The Zukauskas expression was used to estimate  $h_{p_s}$  [49].

$$h_{p_s} = \begin{cases} 0.76 \text{Re}^{0.4} \text{Pr}^{0.37} \frac{k_p}{d} & 0 < \text{Re} \leq 40 \\ 0.52 \text{Re}^{0.5} \text{Pr}^{0.37} \frac{k_p}{d} & 40 < \text{Re} \leq 1000 \\ 0.26 \text{Re}^{0.6} \text{Pr}^{0.37} \frac{k_p}{d} & 1000 < \text{Re} \leq 20000 \end{cases} \quad (17)$$

Effective thermal conductivities of the PCM ( $k_{p_e}$ ) and copper foam ( $k_{s_e}$ ) are determined using formulations proposed by Boomsma and Poulikakos [50]:

$$k_{p_e} = k_{\text{eff}} \Big|_{k_s = 0} \quad (18)$$

$$k_{s_e} = k_{\text{eff}} \Big|_{k_f = 0} \quad (19)$$

Where

$$k_{\text{eff}} = \frac{\sqrt{2}}{2(R_A + R_B + R_C + R_D)} \quad (20)$$

$$R_A = \frac{4d}{(2e^2 + \pi d(1-e))k_s + (4 - 2e^2 - \pi d(1-e))k_f} \quad (21)$$

$$R_B = \frac{(e - 2d)^2}{(e - 2d)e^2 k_s + (2e - 4d - (e - 2d)e^2)k_f} \quad (22)$$

$$R_C = \frac{(\sqrt{2} - 2e)^2}{2\pi d^2 (1 - 2e\sqrt{2})k_s + 2(\sqrt{2} - 2e - \pi d^2 (1 - e\sqrt{2}))k_f} \quad (23)$$

$$R_D = \frac{2e}{e^2 k_s + (4 - e^2)k_f} \quad (24)$$

$$d = \sqrt{\frac{\sqrt{2}(2 - (5/8)e^3\sqrt{2} - 2\varepsilon)}{\pi(3 - 4e\sqrt{2} - e)}}, \quad e=0.339 \quad (25)$$

For pure PCM,  $\varepsilon = 1$ ,  $k_{pe} = k_{se}$  and  $h_{ps}a_{ps}(T_s - T_p) = 0$ .

#### 4.1.5. Numerical method and validation

The numerical model is solved using a finite element analysis with the COMSOL Multiphysics 5.3a software [51]. COMSOL automatically selects the solvers, and then we make the necessary modifications.

To validate the model that predict the melting of pure PCM, the simulation results were compared with experimental data from Kamkari et al. [52]. In their work, a rectangular enclosure filled with lauric acid was investigated. They studied a vertical and inclined enclosure. The comparison of liquid fractions simulated by the current model and experimental results of [52] during melting of Lauric acid at the same initial and boundary conditions for inclination angles of  $0^\circ$  (vertical enclosure) is showed **Figure 12**. The maximum deviations of the current model from [52] is 5%, indicating good validations of this model against experimental.

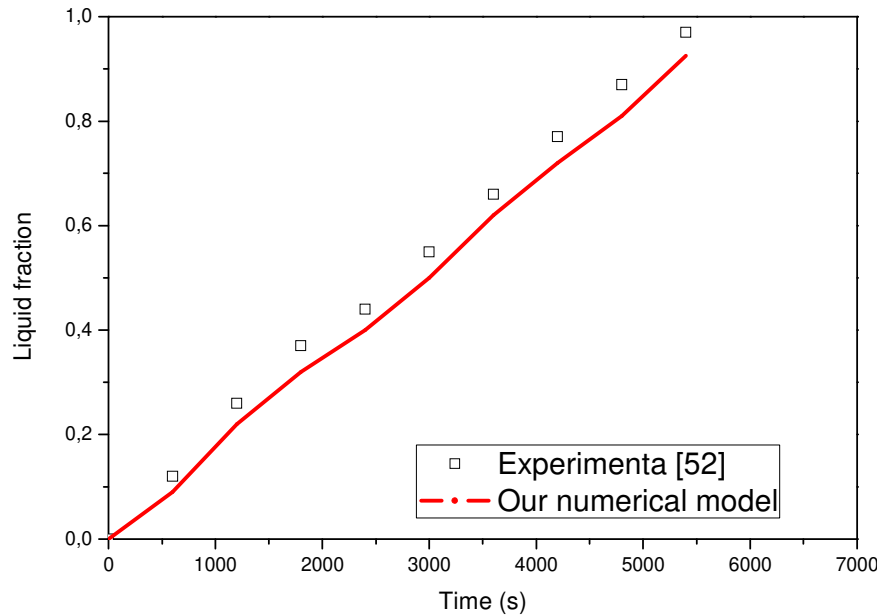


**Figure 12** : Comparison between numerical and experimental

The simulation results of PCM melting embedded in metal foam were validated by comparing the predicted results with the experimental data of the study by Zhao et al. [53]. In the study conducted by Zhao et al. [53], a copper foam sample with dimensions of 200mm, 120mm and 25mm, pores density of 10PPI, and 95% porosity filled with paraffin wax RT58, was heated with a constant heat of  $1600 \text{ W/m}^2$ . The heat loss coefficient generated by the natural convection of air is estimated at about  $3 \text{ W/m}^2$ . The properties of RT58 are given in Table 2. Figure 13 presents a comparison between the evolution of calculated temperature of the PCM at 8 mm away from the copper foam composite bottom and the experimental results. The results show that during the melting process, from 1200s to 4000s, there is a small discrepancy between the numerical results of the present model as well as after the melting process. It can be concluded that the numerical results obtained by the present model is in a good agreement with the experimental data on the whole, and the present model is reliable and reasonable.

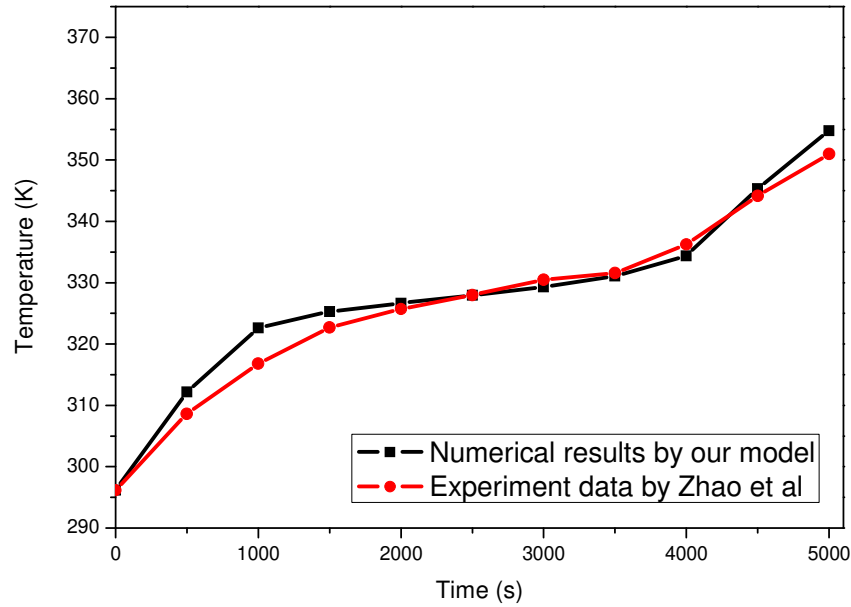


**Figure 13:** Comparison between numerical and experimental

The sensitivity to mesh size has been studied. A mesh decency study carried out on the mesh for three different mesh size. Figure 14 shows the evolution of melt fraction for different mesh size. It was found for all mesh size the melt fraction is varied in a similar manner, with a small difference, between 0-2 percent. With a small mesh size, the solution is more accuracy. For the present study a mesh 64965 elements are used.

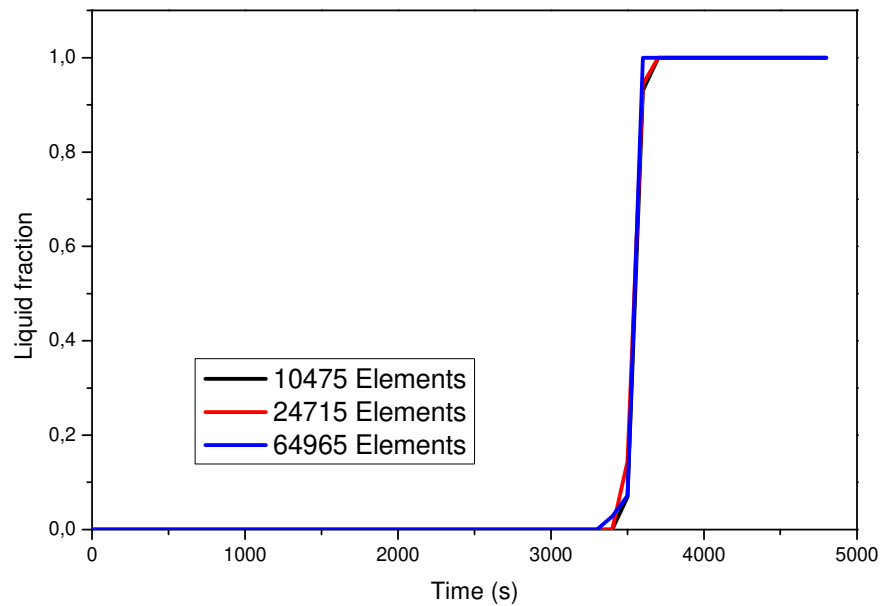


**Figure 14:** Effects of grid on the variation of liquid fraction

## 4.2. Calculation of the amount of PCM required

In order to determine the amount of paraffin RT27 needed to absorb the heat dissipated by the cell, the total heat dissipated by the cell must first be calculated. The amount of heat generated by the cell is the integral of the heat flux density (Eq 36).

$$Q_{Li-ion} = \int_{t_1}^{t_f} \int_S q_{Li-ion} .ds .dt \quad (36)$$

The integral is calculated numerically by the trapezoidal rule by a code developed under Matlab. The mass of PCM is then deduced as follows:

$$Q_{Li-ion} = mCp_{Ps} (T_{ini} - T_{PF}) + mL_f + mCp_l (T_{final} - T_{PF}) \quad (37)$$

$$m = \frac{Q_{Li-ion}}{Cp_{Ps} (T_{ini} - T_{PF}) + L_f + Cp_l (T_{final} - T_{PF})} \quad (38)$$

With  $T_{PF}$  is the maximum temperature not to be exceeded (design temperature), in our case is 27°C. The thickness of the PCM layer surrounding the cell is calculated from the volume of PCM required which is deduced from the mass:

$$e = \Delta r = \sqrt{\frac{V_{PCM} + \pi r_{Li-ion}^2 H_{Li-ion}}{\pi H}} - r_{Li-ion} \quad (39)$$

The calculated thickness is 2.8 mm. The results of this numerical study will be used to set up a BTMS. For this reason, we approximate to 3 mm. The volume is increased by about 7% compared to the calculated volume.

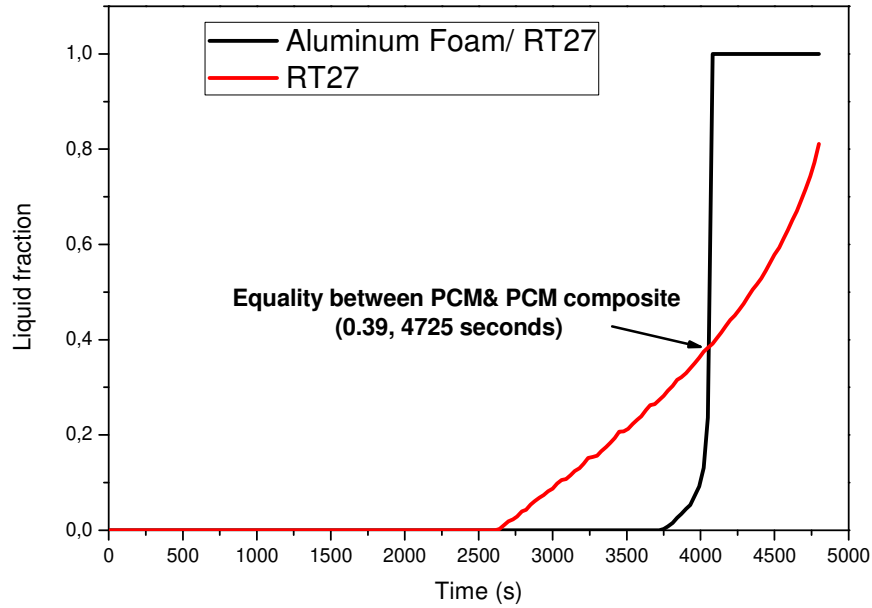


**Figure 15:** Evolution of the liquid fraction

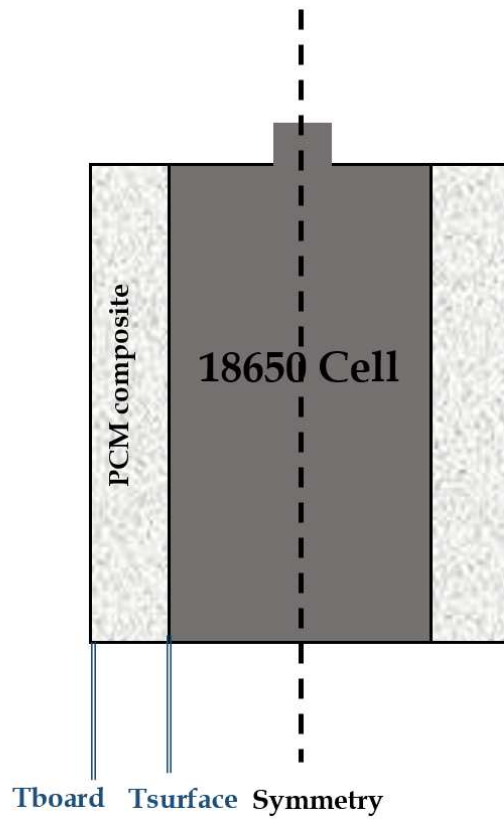


**Figure 16:** Figure illustrates the position of the followed temperatures

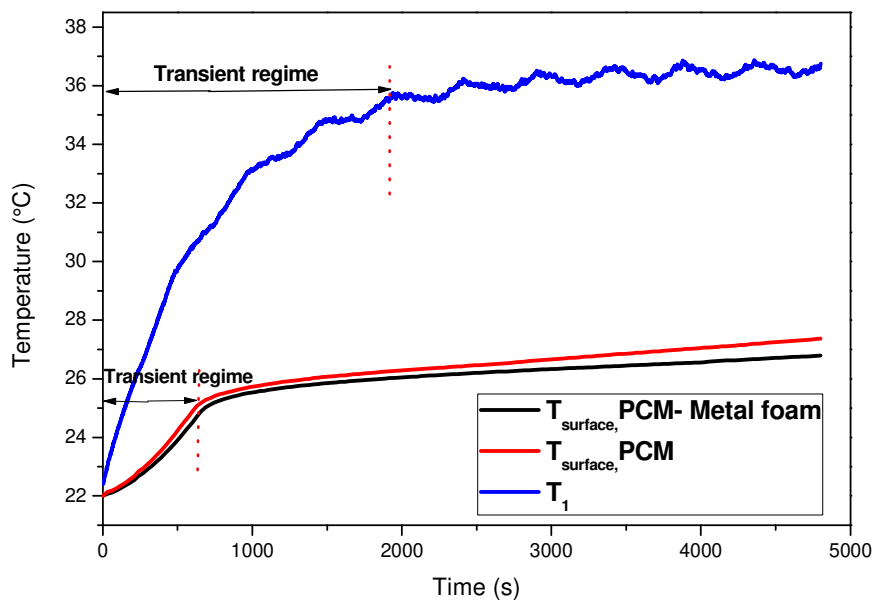


**Figure 17:** Impact of the ad of BTMS on the cell surface temperature

### 4.3. Impact of the addition of BTMS using PCM composite

Figure 14, shows the evolution of the liquid fraction for pure paraffin and for the paraffin/aluminum foam composite. It's can be seen from Figure 15 that the melting starts earlier in the case of a pure PCM (pure paraffin RT27) than in the case of a PCM-metal foam composite (paraffin RT27-aluminum foam). The liquid fraction shows that the pure paraffin has a low solid-liquid kinetic phase change compared to paraffin incorporated in the aluminum foam. The melting of

the pure paraffin starts after 45 minutes and that of the paraffin incorporated in the aluminum foam starts after 62 minutes. Indeed, the addition of a metallic foam improves thermal conductivity and intensifies heat transfer. The low thermal conductivity of pure PCM slows down the heat propagation, which leads to higher temperatures at the battery surface-PCM interface than at the battery surface-PCM composite-metal foam interface. Therefore, pure PCM reaches the melting temperature before the PCM incorporated into the metal foam. At the end of the simulation, we observe that, in the case of thermal management with pure PCM, the PCM is not completely melted. The main reason to use a PCM is its latent heat. On the other hand, the PCM embedded in the metallic foam is completely melted. Indeed, at the end, all the paraffin incorporated in the aluminum foam was in liquid state versus 80% in the case of pure paraffin; hence the importance of incorporating it into a metal foam.

In order to study the impact of PCM composite on the cell temperature and its ability to absorb the energy generated by the cell, the temperature was followed in the cell surface ( $T_{\text{surface}}$ ) and the interface between the adiabatic wall and the PCM composite ( $T_{\text{board}}$ ) like show **Figure 16**. **Figure 17** shows the temperature evolution with and without a thermal management system. The results show that the addition of a pure PCM or a PCM-Metal Foam Composite can significantly reduce the temperature of the cell. It can be seen that the transient time was reduced. Indeed, the duration of transit regime without BTMS is about 2000 seconds and in the case with BTMS is 700 seconds. As soon as PCM melting starts, the cell surface temperature stabilizes around the melting temperature. The gain in time is about 35%. **Figure 18** shows the evolution of the average temperature of the cell surface and the external surface (at the insulation level) in both cases, pure PCM and composite PCM. It can be seen that the use of a PCM/Metal Foam composite is more efficient with a lower cell temperature and a smaller temperature difference. The difference between  $T_{\text{surface}}$  and  $T_{\text{board}}$  is about  $0.2^{\circ}\text{C}$  in the case of Aluminum foam and RT27 composite and about  $1.3^{\circ}\text{C}$  in the case of pure RT27. The addition of aluminum foam intensifies heat transfer and leads to a more uniform temperature field [44,46,54–59]. **Figure 19** and **Figure 20** present respectively the phase fields and the temperature fields of pure RT27 and RT27- Aluminum foam composite for the last 500 seconds. We can see that the temperature field is more uniform in the case of RT27–aluminum foam composite than in the case of pure RT27.

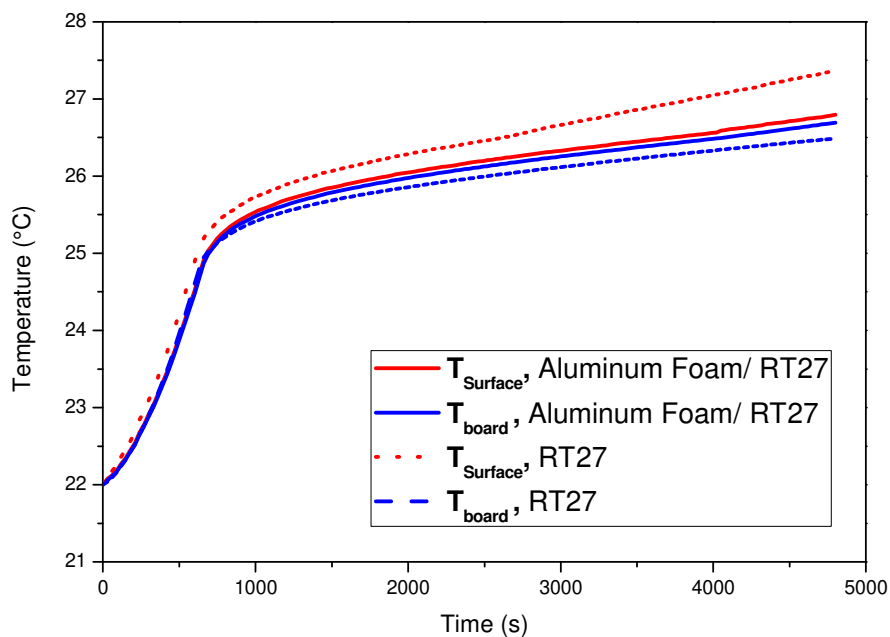


**Figure 18:** Influence of foam addition

#### 4.4. Optimization of the quantity of PCM used

In order to optimize the amount of PCM, the performance of Paraffin RT27/Aluminum Foam composite is evaluated for different thicknesses (2mm, 3mm, 4mm, 5mm and 6mm). **Figure 21** shows a comparison of the evolution of the cell surface temperature for the different thicknesses studied. It can be seen that an underestimation of thickness (mass required) leads to extreme temperatures. The temperature of the cell with a thickness of 2mm reaches 33°C, while the temperature of the cell without a thermal management system reaches 37°C. **Figure 21** shows that the impact of adding more mass of PCMs is greater in the sensitive storage phase. The temperature difference can reach 2°C in the sensitive storage phase while in latent storage it is about 0.5°C. Overall, the addition of extra volume does not have a great influence on the cell temperature. However, the larger the volume of the composite, the heavier the system will be.

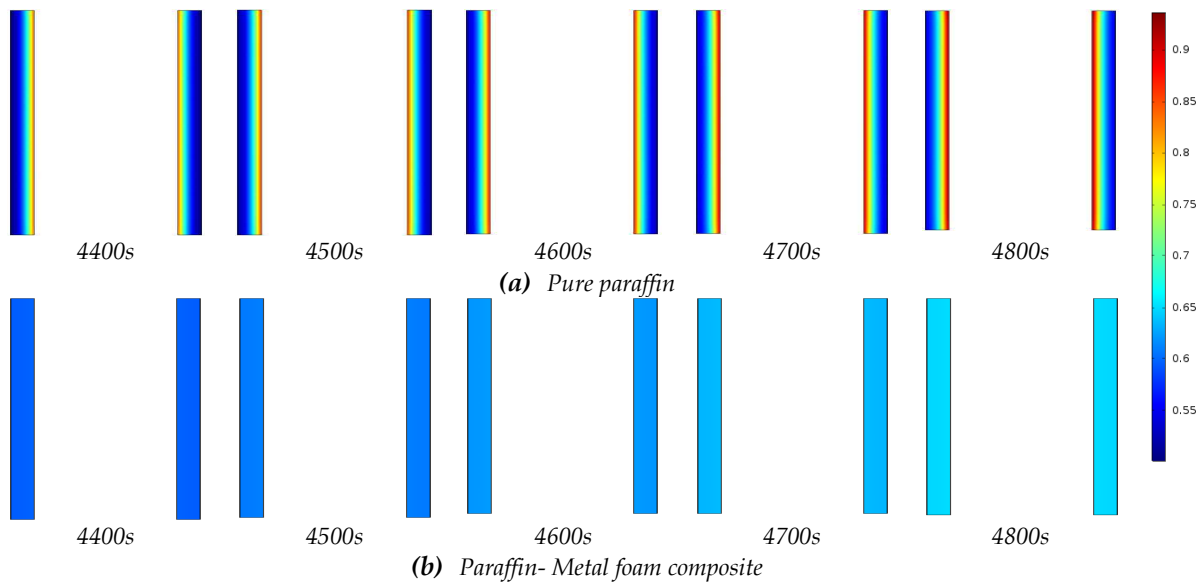


**Figure 19:** Phase field after, (a) pure PCM, (b) PCM- Metal foam

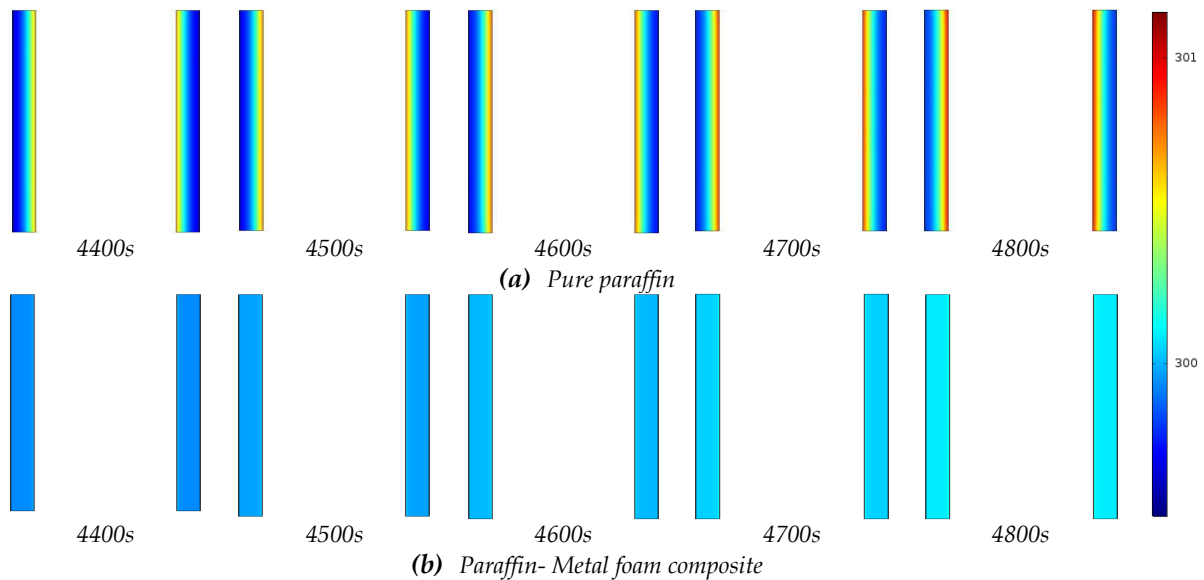


**Figure 20:** Temperature field, (a) pure PCM, (b) PCM- Metal foam

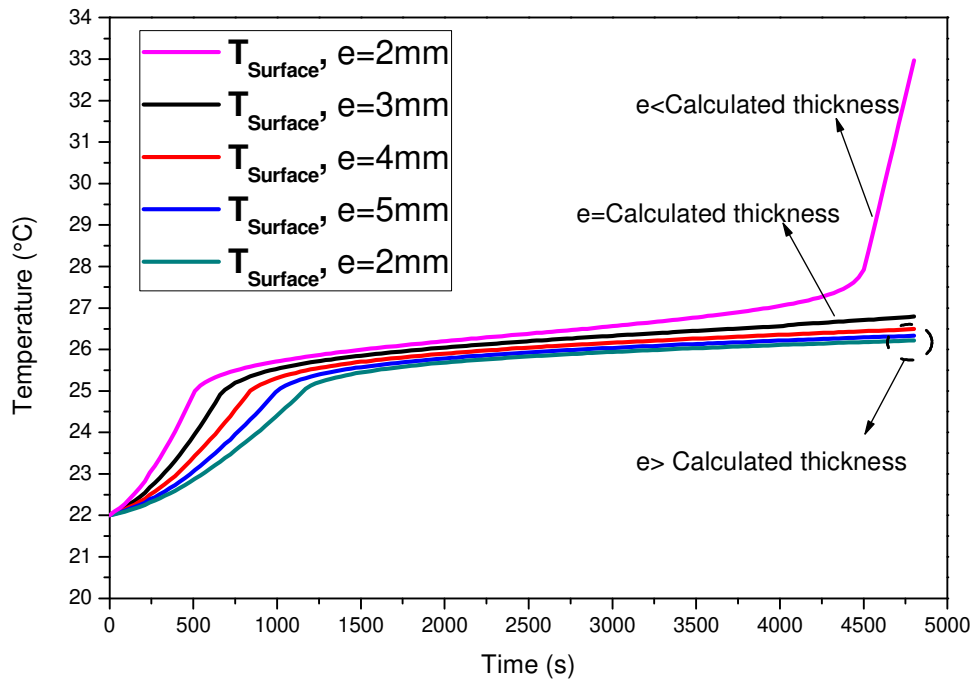


**Figure 21:** Impact of composite thickness on the cell surface temperature

## 5. Conclusion

In this paper a new experimental bench has been developed to study the thermal behavior of a Li-ion battery at cell scale. Li-ion 18650 cell was chosen. A passive thermal management system using an aluminum foam/paraffin RT27 composite was designed and optimized. The aim is to keep the cell below 27 °C while undergoing consecutive charge/discharge cycles. To investigate the efficiency of our BTMS a two-dimensional numerical model based on the enthalpy-porosity model and non-equilibrium equation was developed and validated with experimental data. The result showed that the cell surface temperature depends on several parameters: Current rate, duration of charge and discharge cycle and ambient temperature. It is found that the PCM allows to absorb the heat generated by the cell in latent form in solid-liquid phase change. However, its low thermal conductivity limits its performance. The addition of an aluminum foam allows a more efficient Li-ion cell thermal management of the cell. The optimization study showed that an underestimation of the thickness (mass of PCM required) leads to extreme temperatures. It was -also- found that hat the addition of an extra volume of PCM does not have a great influence on the cell surface temperature.

### Reference:

- [1] G. Jiang, J. Huang, M. Liu, M. Cao, Experiment and simulation of thermal management for a tube-shell Li-ion battery pack with composite phase change material, *Appl. Therm. Eng.* 120 (2017) 1–9. <https://doi.org/10.1016/j.applthermaleng.2017.03.107>.
- [2] L. Ianniciello, P.H. Biwolé, P. Achard, Electric vehicles batteries thermal management systems employing phase change materials, *J. Power Sources.* 378 (2018) 383–403. <https://doi.org/10.1016/j.jpowsour.2017.12.071>.
- [3] A. Pesaran, M. Keyser, G.H. Kim, S. Santhanagopalan, K. Smith, Tools for Designing Thermal Management of Batteries in Electric Drive Vehicles, National Renewable Energy Lab. (NREL), Golden, CO (United States), 2013. <https://doi.org/10.2172/1064502>.

- [4] R. Zhao, S. Zhang, J. Liu, J. Gu, A review of thermal performance improving methods of lithium ion battery: Electrode modification and thermal management system, *J. Power Sources*. 299 (2015) 557–577. <https://doi.org/10.1016/j.jpowsour.2015.09.001>.
- [5] Z. Rao, S. Wang, A review of power battery thermal energy management, *Renew. Sustain. Energy Rev.* 15 (2011) 4554–4571. <https://doi.org/10.1016/j.rser.2011.07.096>.
- [6] B. Zalba, J.M. Marín, L.F. Cabeza, H. Mehling, Review on thermal energy storage with phase change: materials, heat transfer analysis and applications, *Appl. Therm. Eng.* 23 (2003) 251–283. [https://doi.org/10.1016/S1359-4311\(02\)00192-8](https://doi.org/10.1016/S1359-4311(02)00192-8).
- [7] L. Boussaba, S. Makhlof, A. Foufa, G. Lefebvre, L. Royon, vegetable fat: A low-cost bio-based phase change material for thermal energy storage in buildings, *J. Build. Eng.* 21 (2019) 222–229. <https://doi.org/10.1016/j.jobe.2018.10.022>.
- [8] L. Boussaba, A. Foufa, S. Makhlof, G. Lefebvre, L. Royon, Elaboration and properties of a composite bio-based PCM for an application in building envelopes, *Constr. Build. Mater.* 185 (2018) 156–165. <https://doi.org/10.1016/j.conbuildmat.2018.07.098>.
- [9] L. Ianniciello, Etude du comportement thermique d'une batterie électrochimique thermorégulée par matériaux à changement de phase pour le véhicule électrique, thesis, Paris Sciences et Lettres, 2018. <http://www.theses.fr/2018PSLEM020> (accessed April 1, 2020).
- [10] A.A. Pesaran, Battery thermal models for hybrid vehicle simulations, *J. Power Sources*. 110 (2002) 377–382. [https://doi.org/10.1016/S0378-7753\(02\)00200-8](https://doi.org/10.1016/S0378-7753(02)00200-8).
- [11] J. Zhao, Z. Rao, Y. Li, Thermal performance of mini-channel liquid cooled cylinder based battery thermal management for cylindrical lithium-ion power battery, *Energy Convers. Manag.* 103 (2015) 157–165. <https://doi.org/10.1016/j.enconman.2015.06.056>.
- [12] R. Zhao, S. Zhang, J. Gu, J. Liu, S. Carkner, E. Lanoue, An experimental study of lithium ion battery thermal management using flexible hydrogel films, *J. Power Sources*. 255 (2014) 29–36. <https://doi.org/10.1016/j.jpowsour.2013.12.138>.
- [13] H. Hirano, T. Tajima, T. Hasegawa, T. Sekiguchi, M. Uchino, Boiling Liquid Battery Cooling for Electric Vehicle, 2014 IEEE Conf. Expo Transp. Electrification Asia-Pac. ITEC Asia-Pac. (2014) 1–4. <https://doi.org/10.1109/ITEC-AP.2014.6940931>.
- [14] S. Zhang, R. Zhao, J. Liu, J. Gu, Investigation on a hydrogel based passive thermal management system for lithium ion batteries, *Energy*. 68 (2014) 854–861. <https://doi.org/10.1016/j.energy.2014.03.012>.
- [15] R. Rizk, H. Louahlia, H. Gualous, P. Schaetzel, Passive Cooling of High Capacity Lithium-Ion batteries, 2018 IEEE Int. Telecommun. Energy Conf. IN **TEL** (2018) 1–4. <https://doi.org/10.1109/INTLEC.2018.8612368>.
- [16] N. Putra, B. Ariantara, R.A. Pamungkas, Experimental investigation on performance of lithium-ion battery thermal management system using flat plate loop heat pipe for electric vehicle application, *Appl. Therm. Eng.* 99 (2016) 784–789. <https://doi.org/10.1016/j.applthermaleng.2016.01.123>.
- [17] Q. Wang, B. Jiang, Q.F. Xue, H.L. Sun, B. Li, H.M. Zou, Y.Y. Yan, Experimental investigation on EV battery cooling and heating by heat pipes, *Appl. Therm. Eng.* 88 (2015) 54–60. <https://doi.org/10.1016/j.applthermaleng.2014.09.083>.
- [18] J. Rhi, Battery Thermal Management System of Future Electric Vehicles with Loop Thermosyphon, in: n.d. [https://scholar.google.com/scholar\\_lookup?title=Battery%20thermal%20management%20system%20of%20future%20electric%20vehicles%20with%20loop%20thermosyphon&author=Rhi%20Jang&publication\\_year=2010](https://scholar.google.com/scholar_lookup?title=Battery%20thermal%20management%20system%20of%20future%20electric%20vehicles%20with%20loop%20thermosyphon&author=Rhi%20Jang&publication_year=2010) (accessed April 6, 2020).
- [19] G. Swanepoel, Thermal management of hybrid electrical vehicles using heat pipes, Thesis, Stellenbosch : Stellenbosch University, 2001. <https://scholar.sun.ac.za:443/handle/10019.1/52564> (accessed April 6, 2020).
- [20] S.A. Hallaj, J.R. Selman, A Novel Thermal Management System for Electric Vehicle Batteries Using Phase-Change Material, *J. Electrochem. Soc.* 147 (2000) 3231. <https://doi.org/10.1149/1.1393888>.

- [21] S.A. Khateeb, M.M. Farid, J.R. Selman, S. Al-Hallaj, Design and simulation of a lithium-ion battery with a phase change material thermal management system for an electric scooter, *J. Power Sources*. 128 (2004) 292–307. <https://doi.org/10.1016/j.jpowsour.2003.09.070>.
- [22] S.A. Khateeb, S. Amiruddin, M. Farid, J.R. Selman, S. Al-Hallaj, Thermal management of Li-ion battery with phase change material for electric scooters: experimental validation, *J. Power Sources*. 142 (2005) 345–353. <https://doi.org/10.1016/j.jpowsour.2004.09.033>.
- [23] A. Mills, S. Al-Hallaj, Simulation of passive thermal management system for lithium-ion battery packs, *J. Power Sources*. 141 (2005) 307–315. <https://doi.org/10.1016/j.jpowsour.2004.09.025>.
- [24] R. Sabbah, R. Kizilel, J.R. Selman, S. Al-Hallaj, Active (air-cooled) vs. passive (phase change material) thermal management of high power lithium-ion packs: Limitation of temperature rise and uniformity of temperature distribution, *J. Power Sources*. 182 (2008) 630–638. <https://doi.org/10.1016/j.jpowsour.2008.03.082>.
- [25] X. Duan, G.F. Naterer, Heat transfer in phase change materials for thermal management of electric vehicle battery modules, *Int. J. Heat Mass Transf.* 53 (2010) 5176–5182. <https://doi.org/10.1016/j.ijheatmasstransfer.2010.07.044>.
- [26] C.-V. Hémerly, Etudes des phénomènes thermiques dans les batteries Li-ion., phdthesis, Université de Grenoble, 2013. <https://tel.archives-ouvertes.fr/tel-00968666> (accessed March 2, 2020).
- [27] M.M. El idi, M. Karkri, M. Kraiem, Preparation and effective thermal conductivity of a Paraffin/Metal Foam composite, *J. Energy Storage*. (2020) 102077. <https://doi.org/10.1016/j.est.2020.102077>.
- [28] M.M. EL IDI, M. Karkri, M.A. Tankari, C. Larouci, T. Azib, G. Levebre, Caractérisation du comportement thermique des batteries Li-ion en vue d'une gestion optimale passive, in: *Congrès Annu. Société Fr. Therm.* 2020, Belfort, France, 2020. <https://doi.org/10.25855/SFT2020-148>.
- [29] W.Q. Li, Z.G. Qu, Y.L. He, Y.B. Tao, Experimental study of a passive thermal management system for high-powered lithium ion batteries using porous metal foam saturated with phase change materials, *J. Power Sources*. 255 (2014) 9–15. <https://doi.org/10.1016/j.jpowsour.2014.01.006>.
- [30] Z. Ling, J. Chen, X. Fang, Z. Zhang, T. Xu, X. Gao, S. Wang, Experimental and numerical investigation of the application of phase change materials in a simulative power batteries thermal management system, *Appl. Energy*. 121 (2014) 104–113. <https://doi.org/10.1016/j.apenergy.2014.01.075>.
- [31] Y. Lv, X. Yang, G. Zhang, Durability of phase-change-material module and its relieving effect on battery deterioration during long-term cycles, *Appl. Therm. Eng.* 179 (2020) 115747. <https://doi.org/10.1016/j.applthermaleng.2020.115747>.
- [32] C. Xiao, G. Zhang, Z. Li, X. Yang, Custom design of solid–solid phase change material with ultra-high thermal stability for battery thermal management, *J. Mater. Chem. A*. 8 (2020) 14624–14633. <https://doi.org/10.1039/D0TA05247G>.
- [33] M.A. Bamdezh, G.R. Molaeimanesh, S. Zanganeh, Role of foam anisotropy used in the phase-change composite material for the hybrid thermal management system of lithium-ion battery, *J. Energy Storage*. 32 (2020) 101778. <https://doi.org/10.1016/j.est.2020.101778>.
- [34] M.A. Bamdezh, G.R. Molaeimanesh, Impact of system structure on the performance of a hybrid thermal management system for a Li-ion battery module, *J. Power Sources*. 457 (2020) 227993. <https://doi.org/10.1016/j.jpowsour.2020.227993>.
- [35] M. Mehrabi-Kermani, E. Houshfar, M. Ashjaee, A novel hybrid thermal management for Li-ion batteries using phase change materials embedded in copper foams combined with forced-air convection, *Int. J. Therm. Sci.* 141 (2019) 47–61. <https://doi.org/10.1016/j.ijthermalsci.2019.03.026>.
- [36] H. Zhang, X. Wu, Q. Wu, S. Xu, Experimental investigation of thermal performance of large-sized battery module using hybrid PCM and bottom liquid cooling configuration, *Appl. Therm. Eng.* 159 (2019) 113968. <https://doi.org/10.1016/j.applthermaleng.2019.113968>.

- [37] S. Hekmat, G.R. Molaeimanesh, Hybrid thermal management of a Li-ion battery module with phase change material and cooling water pipes: An experimental investigation, *Appl. Therm. Eng.* 166 (2020) 114759. <https://doi.org/10.1016/j.applthermaleng.2019.114759>.
- [38] M. Mashayekhi, E. Houshfar, M. Ashjaee, Development of hybrid cooling method with PCM and Al<sub>2</sub>O<sub>3</sub> nanofluid in aluminium minichannels using heat source model of Li-ion batteries, *Appl. Therm. Eng.* 178 (2020) 115543. <https://doi.org/10.1016/j.applthermaleng.2020.115543>.
- [39] Y. Lv, G. Liu, G. Zhang, X. Yang, A novel thermal management structure using serpentine phase change material coupled with forced air convection for cylindrical battery modules, *J. Power Sources*. 468 (2020) 228398. <https://doi.org/10.1016/j.jpowsour.2020.228398>.
- [40] T. Zhang, C. Gao, Q. Gao, G. Wang, M. Liu, Y. Guo, C. Xiao, Y.Y. Yan, Status and development of electric vehicle integrated thermal management from BTM to HVAC, *Appl. Therm. Eng.* 88 (2015) 398–409. <https://doi.org/10.1016/j.applthermaleng.2015.02.001>.
- [41] Y. Li, Y. Du, T. Xu, H. Wu, X. Zhou, Z. Ling, Z. Zhang, Optimization of thermal management system for Li-ion batteries using phase change material, *Appl. Therm. Eng.* 131 (2018) 766–778. <https://doi.org/10.1016/j.applthermaleng.2017.12.055>.
- [42] R. Rizk, H. Louahlia, H. Gualous, P. Schaezel, G. Alcicek, Experimental analysis on Li-ion battery local heat distribution, *J. Therm. Anal. Calorim.* 138 (2019) 1557–1571. <https://doi.org/10.1007/s10973-019-08283-9>.
- [43] R. Rizk, H. Louahlia, H. Gualous, P. Schaezel, Experimental analysis and transient thermal modelling of a high capacity prismatic lithium-ion battery, *Int. Commun. Heat Mass Transf.* 94 (2018) 115–125. <https://doi.org/10.1016/j.icheatmasstransfer.2018.03.018>.
- [44] E.I. Mohamed Moussa, M. Karkri, A numerical investigation of the effects of metal foam characteristics and heating/cooling conditions on the phase change kinetic of phase change materials embedded in metal foam, *J. Energy Storage*. 26 (2019) 100985. <https://doi.org/10.1016/j.est.2019.100985>.
- [45] R. Viswanath, Y. Jaluria, A Comparison of Different Solution Methodologies for Melting and Solidification Problems in Enclosures, *Numer. Heat Transf. Part B Fundam.* 24 (1993) 77–105. <https://doi.org/10.1080/10407799308955883>.
- [46] M. Moussa EL IDI, M. Karkri, Heating and cooling conditions effects on the kinetic of phase change of PCM embedded in metal foam, *Case Stud. Therm. Eng.* (2020) 100716. <https://doi.org/10.1016/j.csite.2020.100716>.
- [47] Y. Yao, H. Wu, Z. Liu, Z. Gao, Pore-scale visualization and measurement of paraffin melting in high porosity open-cell copper foam, *Int. J. Therm. Sci.* 123 (2018) 73–85. <https://doi.org/10.1016/j.ijthermalsci.2017.09.011>.
- [48] P.H. Biwole, D. Groulx, F. Souayfane, T. Chiu, Influence of fin size and distribution on solid-liquid phase change in a rectangular enclosure, *Int. J. Therm. Sci.* 124 (2018) 433–446. <https://doi.org/10.1016/j.ijthermalsci.2017.10.038>.
- [49] Z. A, Heat transfer from tubes in crossflow, 18 (1987) 87–139.
- [50] K. Boomsma, D. Poulikakos, On the effective thermal conductivity of a three-dimensionally structured fluid-saturated metal foam, *Int. J. Heat Mass Transf.* 44 (2001) 827–836. [https://doi.org/10.1016/S0017-9310\(00\)00123-X](https://doi.org/10.1016/S0017-9310(00)00123-X).
- [51] COMSOL: Multiphysics Software for Optimizing Designs, COMSOL Multiphysics®. (n.d.). <https://www.comsol.fr/> (accessed February 19, 2020).
- [52] B. Kamkari, H. Shokouhmand, F. Bruno, Experimental investigation of the effect of inclination angle on convection-driven melting of phase change material in a rectangular enclosure, *Int. J. Heat Mass Transf.* 72 (2014) 186–200. <https://doi.org/10.1016/j.ijheatmasstransfer.2014.01.014>.
- [53] C.Y. Zhao, W. Lu, Y. Tian, Heat transfer enhancement for thermal energy storage using metal foams embedded within phase change materials (PCMs), *Sol. Energy*. 84 (2010) 1402–1412. <https://doi.org/10.1016/j.solener.2010.04.022>.
- [54] E.I. Mohamed Moussa, M. Karkri, A numerical investigation of the effects of metal foam characteristics and heating/cooling conditions on the phase change kinetic of phase change

- materials embedded in metal foam, *J. Energy Storage*. 26 (2019) 100985.  
<https://doi.org/10.1016/j.est.2019.100985>.
- [55] M.M. EL IDI, M. Karkri, Etude numérique de stockage d'énergie thermique dans un composite : mousses métalliques/matériaux à changement de phase, in: Congrès Fr. Therm. SFT 2019, Nantes, France, 2019. <https://hal.archives-ouvertes.fr/hal-02399163> (accessed February 20, 2020).
- [56] M.M. EL IDI, M. Karkri, Méthode inverse pour la détermination expérimentale des propriétés thermophysiques des matériaux à changement de phase, in: Congrès Fr. Therm. SFT 2018, PAU, France, 2018. <https://hal.archives-ouvertes.fr/hal-02402478> (accessed July 14, 2020).
- [57] M.M. EL IDI, M. KARKRI, M.A. TANKARI, C. LAROUCI, T. AZIB, G. LEVEBRE, Thermal management of Li-ion batteries using PCM-Metal foam composite: Experimental and numerical investigations, in: *Ann. Congrès Annu. Société Fr. Therm.* 2020, Belfort, France, n.d.: p. 8.  
<https://doi.org/10.25855/SFT2020-148>.
- [58] M.M. EL IDI, M. Karkri, M.A. Tankari, C. Larouci, T. Azib, G. Levebre, Thermal management of Li-ion batteries using PCM-Metal foam composite: Experimental and numerical investigations, in: *Congrès Annu. Société Fr. Therm.* 2020, Belfort, France, 2020.  
<https://doi.org/10.25855/SFT2020-148>.
- [59] M.M. EL IDI, M. KARKRI, Melting and solidification behavior of paraffin embedded in metal foam, *J. Sustain. Urban. Regen.* 2 (2019) 1–10.